Accepted Manuscript

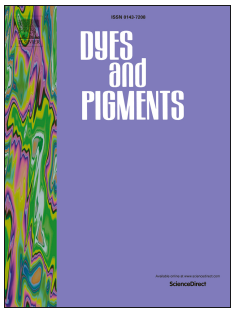

A mitochondria-targeted ratiometric fluorescence sensor for the detection of hypochlorite in living cells

Wei Wang, Jun-Ya Ning, Jin-Ting Liu, Jun-Ying Miao, Bao-Xiang Zhao

PII: S0143-7208(19)31253-7

DOI: https://doi.org/10.1016/j.dyepig.2019.107708

Article Number: 107708

Reference: DYPI 107708

To appear in: *Dyes and Pigments*

Received Date: 31 May 2019

Revised Date: 4 July 2019

Accepted Date: 9 July 2019

Please cite this article as: Wang W, Ning J-Y, Liu J-T, Miao J-Y, Zhao B-X, A mitochondria-targeted ratiometric fluorescence sensor for the detection of hypochlorite in living cells, *Dyes and Pigments* (2019), doi: https://doi.org/10.1016/j.dyepig.2019.107708.

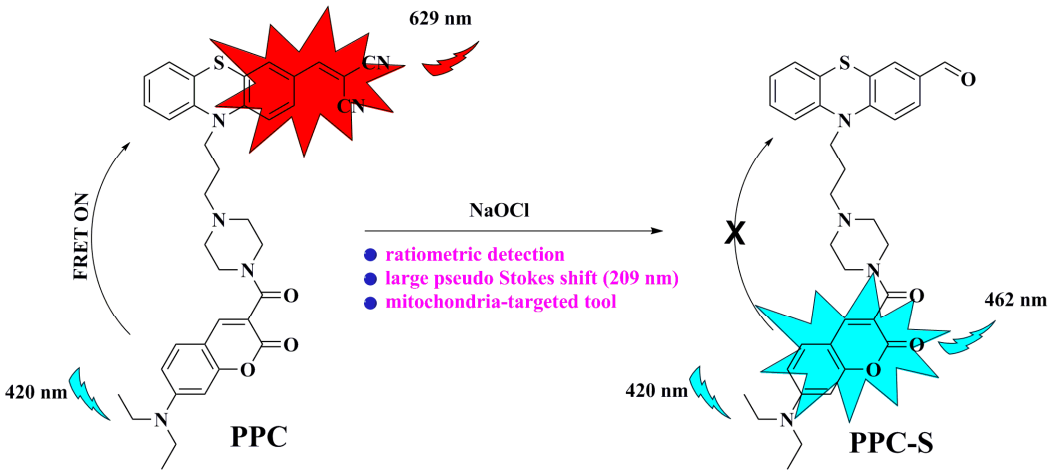

A mitochondria-targeted ratiometric fluorescence sensor for the detection of hypochlorite in living cells

Wei Wang[a,] , Jun-Ya Ning[b,] , Jin-Ting Liu[a], Jun-Ying Miao[b], Bao-Xiang Zhao[a*]

[a]*Institute of Organic Chemistry, School of Chemistry and Chemical Engineering, Shandong University, Jinan 250100, PR China*

[b]*Institute of Developmental Biology, School of Life Science, Shandong University, Jinan 250100, PR China*

*Corresponding author. Tel.: +86 531 7862972268; fax: +86 531 7862972268.

E-mail address: bxzhao@sdu.edu.cn.

Abstract

A new fluorescence probe based on phenothiazine-coumarin platform was rationally designed and developed for the detection of hypochlorite in a ratiometric manner in aqueous solution and living cells. The probe possessed a large pseudo Stokes shift (209 nm) and lager gap between two emissions (462/629 nm), which should avail to perform more accurate detection. The probe could respond to hypochlorite with selectivity, sensitivity and celerity. Moreover, the probe was successfully used for imaging endogenous hypochlorite in mitochondria of RAW264.7 macrophage cells with high sensitivity.

Keywords: Fluorescence; FRET; Stokes shift; Ratiometric; Endogenous hypochlorite; Mitochondria-targeted.

1. Introduction

As one of reactive oxygen species (ROS) [1, 2], hypochlorous acid/hypochlorite ($HOCl/OCl^-$) plays an essential role in our daily life. $HOCl/OCl^-$ is usually related to various diseases such as lung injury, asthma, arthritis and even some cancers [3-6]. Endogenous $HOCl/OCl^-$ is generated from chloride ion and hydrogen peroxide in the myeloperoxidase (MPO)-catalyzed reaction and plays an important role in resisting multifarious pathogens bacteria and pathogens in organism [7-9]. Hence, developing reliable methods to detect $HOCl/OCl^-$ quantitatively is urgent. Fortunately, fluorescent probes have many prominent advantages in quantitative detection such as low cost, high sensitivity, excellent selectivity and fast response [10-17]. In the past few years, various fluorescence probes have been designed on different fluorophores such as cyanine [18], BODIPY [19, 20], coumarin [21, 22], rhodamine [23, 24], phenothiazine [25, 26]. But most of them were intensity-based fluorescence probes which were usually affected by many factors such as instrumental deviation and environment variations. On the contrary, ratiometric fluorescence probes could sufficiently overcome these shortcomings by means of the fluorescence intensity ratios of two emission peaks [27, 28]. Therefore, ratiometric fluorescence probes based on different platforms, including FRET [29-32], TBET [33, 34], and ICT [35-37], have remained a focus of extensive research activity. Moreover, organelle-targeted fluorescence probes for the selective detection of chemical species were another intriguing direction. So far, some ratiometric and organelle-targeted fluorescence probes for the detection of $HOCl/OCl^-$ have been reported [38, 39], but most of them existed widespread drawbacks in Stokes shifts, response time and organelle-targeted capacity. Therefore, rational design

of ratiometric and organelle-targeted fluorescence probes for HOCl/OCl^- based on new platforms and fluorophores is still challenging.

Phenothiazine and its derivatives as fluorophores showed many outstanding advantages such as high fluorescence quantum yield, large pseudo Stokes shift, excellent photostability and the ability of being chemical modified. So some fluorescence probes for the detection of HOCl/OCl^- based on phenothiazine derivatives have been reported recent years [25, 26]. However, almost all these phenothiazine-based fluorescence probes for the detection of HOCl/OCl^- were based ICT platform and single emission. To date, the Förster resonance energy transfer (FRET) mechanism has not been applied to phenothiazine-based fluorescence probes for the detection of HOCl/OCl^-. As a continuation of our efforts directed toward the development of FRET-based ratiometric fluorescence probes [29-32], we designed a new phenothiazine-based ratiometric fluorescence probe (named **PPC**) for the detection of HOCl/OCl^- in aqueous solution. Probe **PPC** showed excellent selectivity toward HOCl/OCl^-. The limit of detection was calculated to be as low as 0.321 μM, suggesting the high sensitivity. Importantly, probe **PPC** could respond to HOCl/OCl^- shortly (within 40 s). What's more, probe **PPC** was successfully used for the fluorescence imaging of endogenous HOCl/OCl^- in mitochondria of RAW264.7 macrophage cells with high sensitivity.

2. Experimental

2.1 Equipment and materials

^{1}H NMR (300 MHz) and ^{13}C NMR (100 or 75 MHz) was recorded on a Bruker Avance 300 spectrometer or Bruker Avance 400 spectrometer with DMSO-d_6 as a solvent and TMS as an internal standard. Mass spectra were recorded using a Q-TOF6510 spectrograph (Agilent). Melting points

were recorded by an XD-4 digital micro melting point apparatus. UV-vis spectra were obtained by a Hitachi U-4100 spectrophotometer. pH was measured by a PHS-3C pH meter. All fluorescence spectra were recorded by the excitation at 420 nm.

2.2 Preparation of test solutions

The probe was dissolved in DMSO to form a stock solution (10^{-3} M). The test systems were prepared by adding 50 μl stock solution into a 10 ml volumetric flask and diluting it to 10 ml with phosphate buffer (pH = 7.4). Various testing species were added with a micropipette to the above test systems. All these test solutions would be measured immediately.

2.3 Preparation of ROS and RNS

Various ROS (0.125 mM) and RNS (0.125 mM) were prepared by the following methods. NaClO, H_2O_2, *t*-BuOOH solutions were obtained by diluting their stock solution with twice-distilled water. F^-, Cl^-, Br^-, I^-, CO_3^{2-}, SO_4^{2-}, AcO^-, HPO_3^{2-}, NO_2^-, Na^+, Al^{3+}, Mg^{2+}, Cu^{2+}, Fe^{2+}, Zn^{2+}, Fe^{3+}, Ca^{2+} solutions were prepared by dissolving corresponding inorganic salts in twice-distilled water. Hydroxyl radical (•OH) was produced by Fenton reaction on mixing $FeSO_4 \cdot 7H_2O$ with H_2O_2. Nitric oxide (NO) was prepared by potassium nitroprusside. *Tert*-butoxy radical (*t*-BuO•) [30], peroxynitrite ($ONOO^-$) [40], superoxide ($^-O_2$) [41], single oxygen ($^1O_2$) [42] were produced as the reported methods.

Scheme 1

2.4 Synthesis of

10-(3-(4-(7-(diethylamino)-2-oxo-2H-chromene-3-carbonyl)piperazin-1-yl)propyl)-10H-phenothiazine-3-carbaldehyde (**PPC**).

Compound **2-4**, **PPC-S**, Donor and Acceptor were synthesized according to literature [43, 44] (Scheme S1).

10-(3-(4-(7-(Diethylamino)-2-oxo-2H-chromene-3-carbonyl)piperazin-1-yl)propyl)-10H-phenothiazine-3-carbaldehyde (**PPC-S**) (300 mg, 0.50 mmol) and malononitrile (33 mg, 0.50 mmol) were dissolved in absolute ethanol (30 ml). The reaction mixture was heated and kept refluxing for 2 h. The solvent was removed under reduced pressure and the crude product was purified by column chromatography on silica gel (CH_2Cl_2: CH_3OH= 10: 1) to give **PPC** (205.3 mg) in 63.68% yield (Scheme 1). Red solid, m.p.: 142-144 □; ^{1}H NMR (300 MHz, DMSO-d_6): δ = 1.13 (t, *J* = 6.9 Hz, 6H), 1.83 (t, *J* = 6.3 Hz, 2H), 2.34 (s, 4H), 2.41-2.51 (m, 2H), 3.24 (s, 2H), 3.41-3.48 (m, 6H), 4.04 (t, *J* = 6.9 Hz, 2H), 6.54 (d, *J* = 2.4 Hz, 1H), 6.73 (dd, J_1 = 5.7 Hz, J_2 = 3.3 Hz, 1H), 7.02 (t, *J* = 7.4 Hz 1H), 7.16 (d, *J* = 7.8 Hz, 2H), 7.21-7.27 (m, 2H), 7.48 (d, *J* = 9 Hz, 1H), 7.68 (d, *J* = 2.1 Hz, 1H), 7.82 (dd, J_1 = 5.4 Hz, J_2 = 3.3 Hz 1H), 7.92 (s, 1H), 8.23 (s, 1H). ^{13}C NMR (100 MHz, DMSO-d_6): 164.34, 159.21, 158.81, 157.02, 151.66, 150.49, 143.91, 142.57, 132.36, 130.49, 129.21, 128.59, 127.74, 125.87, 124.53, 123.40, 122.14, 117.22, 116.65, 116.17, 115.41, 114.55, 109.82, 107.59, 96.80, 76.47, 54.64, 46.80, 45.55, 44.63, 23.88, 12.76. HRMS: m/z calculated for $[C_{37}H_{36}N_6O_3S + H]^+$: 645.2642, found 645.2458 (Fig. S1-4).

Acceptor: ^{1}H NMR (300 MHz, $CDCl_3$): δ = 2.09-2.19 (m, 2H), 3.76 (t, *J* = 6.3 Hz, 2H), 4.13 (t, *J* = 6.8 Hz, 2H), 7.02-7.06 (m, 1H), 7.16-7.29 (m, 4H), 7.71 (d, *J* = 2.4 Hz, 1H), 7.85 (dd, J_1 = 3.3 Hz, J_2 = 5.4, 1H), 8.27 (s, 1H). ^{13}C NMR (75 MHz, DMSO-d_6): 158.80, 149.79, 141.97, 131.70,

128.94, 128.16, 127.40, 125.62, 124.19, 123.40, 121.97, 116.64, 115.73, 114.84, 113.96, 76.46, 44.14, 42.42, 28.83 (Fig. S5, 6).

2.5 Culture and imaging of HOCl/OCl^- in RAW264.7cells

RAW264.7 macrophage cells were cultured in Dulbecco's modified Eagle's medium (DMEM) containing 10% fetal bovine serum in an atmosphere of 5% CO_2 and 95% air at 37 ^oC. RAW264.7 macrophage cells were stimulated by 1 μg/ml lipopolysaccharides (LPS) for 12 h and then incubated with probe **PPC** (2 μM) for 30 min. After cells were washed three times with PBS, images were obtained by a confocal microscope (LSM 700) at 405 nm excitation. The images of cells were collected at emission channels of 405-555 nm (blue channel) and 560-700 nm (red channel).

3. Results and discussion

Scheme 2

3.1. Selectivity of probe **PPC** toward HOCl/OCl^- by fluorescence method

The selectivity of probe **PPC** toward HOCl/OCl^- was verified in aqueous solution (10 mM PBS with 1 mM Triton X-100, pH = 7.4). The emission spectra of probe **PPC** in the presence of various species (vacant, H_2O_2, KO_2, NO, $^1O_2$, *t*-BuOOH, *t*-BuOO•, •OH, $ONOO^-$, Na^+, Al^{3+}, Zn^{2+}, Ca^{2+}, Fe^{3+}, Fe^{2+}, Cu^{2+}, Mg^{2+}, F^-, Cl^-, Br^-, I^-, CO_3^{2-}, SO_4^{2-}, NO_2^-, AcO^-, HPO_3^{2-}, HOCl/OCl^-, Cys, GSH, Hcy, H_2S and HSO_3^- were obtained (Fig. 1). After the addition of HOCl/OCl^-, the emission peak at 629 nm decreased obviously and the emission peak at 462 nm increased remarkably, suggesting that the FRET process of probe **PPC** was suppressed. However, after the addition of other ROS/RNS, cations, anions and bio-thiols, hardly any obvious changes were observed. The reason for this phenomenon is

the destruction of the "C=C" double bond in probe **PPC** by HOCl/OCl^-. In addition, the anti-interference ability of probe **PPC** for the detection of HOCl/OCl^- in the presence of other species (Zn^{2+}, Na^+, K^+, Cu^{2+}, Ca^{2+}, H_2O_2, NO, •OH, KO_2, *t*-BuOO•) was evaluated (Fig. S7). Compared with the emission band of probe **PPC** alone, in the presence of HOCl/OCl^- and other ROS, obvious changes of the emission band of probe **PPC** at 629 nm and 462 nm could be observed. The decrease in fluorescence intensity at 629 nm and the increase in fluorescence intensity at 462 nm gave rise to obvious enhancement of the ratio of fluorescence intensity (I_{462}/I_{629}). Therefore, probe **PPC** showed outstanding selectivity and anti-interference ability, which should offer a powerful tool for the specific detection of endogenous HOCl/OCl^- in complex physiological environment.

Fig. 1

3.2. Time, pH and fluorescence lifetimes dependence of probe **PPC** toward HOCl/OCl^-

The response time of probe **PPC** toward HOCl/OCl^- was evaluated (Fig. S8). Upon addition of HOCl/OCl^- to the solution of the probe, the color of solution changed from red to pale yellow immediately. The reaction could finish within 40 s. The outstanding response of probe **PPC** to HOCl/OCl^- was among the fastest ones (Table S1) [45-55], which meets well the requirement of real-time detection. The impacts of pH on the detection of HOCl/OCl^- are very important, especially for cell image. Therefore, fluorescence of the probe and its response toward HOCl/OCl^- in different pH were measured (Fig. S9 a). The fluorescence intensity ratios (I_{462}/I_{629}) of the probe remained stable over a wide range of pH (pH = 4-9). In addition, in the presence of HOCl/OCl^-, the fluorescence intensity ratios (I_{462}/I_{629}) of the solution were no obvious change in the range of pH 5-8.

The mild surroundings should suit bioimaging in living cells. Fluorescence lifetimes of probe **PPC** and **PPC-S** were respectively evaluated and showed 2.50 ns and 1.03 ns (Fig. S9 b).

3.3 Fluorescence titration of HOCl/NaOCl with **PPC**

Titration experiments were conducted by adding $HOCl/OCl^-$ (0-6.5 equiv.) into the solution of the probe (5 μM) (Fig. 2a). As $HOCl/OCl^-$ varied from 0 to 6.5 equiv., the fluorescence intensity at 629 nm decreased and the fluorescence intensity at 462 nm increased gradually. Compared with other fluorescent probes (Table S1) [45-55], the larger pseudo Stokes shift (209 nm) from 629 nm to 420 nm of the probe and the lager gap between two emissions implied that the more detection accuracy could be achieved. What's more, an excellent linearity was obtained between the fluorescence intensity ratios ($I_{462\ nm}/I_{629\ nm}$) and the concentrations of $HOCl/OCl^-$ in the range of 0 to 6.5 equiv. (Fig. 2b). Then the limit of detection was calculated with the established formula (LOD = 3σ/slope). The limit of detection for $HOCl/OCl^-$ was evaluated to be as low as 0.321 μM, suggesting probe **PPC** had excellent sensitivity toward $HOCl/OCl^-$. Therefore, the probe could be used to detect low concentrations of endogenous $HOCl/OCl^-$ in living cells.

Fig. 2

3.4 Absorption spectra of probe **PPC** titrated with $HOCl/OCl^-$ and excitation spectra of probe **PPC**

The absorption spectra of probe **PPC** showed two peaks at 412 nm and 466 nm, which could be attributed to the donor (coumarin) and the acceptor (phenothiazine) moiety, respectively (Fig. S10 a). With addition of increasing amount of $HOCl/OCl^-$ (0-6 equiv.), the absorption band of the acceptor moiety at 466 nm decreased gradually and that of the donor moiety remained unchanged.

These results suggested that the structure of the acceptor unit was destroyed and the donor unit was unchanged in the presence of HOCl/OCl^-. The excitation spectra of probe **PPC** also be measured and showed a main excitation scope from 350 nm to 550 nm (Fig. S10 b).

3.5 Calculation of energy transfer efficiency (ETE) and fluorescence quantum yield (Φ)

To evaluate energy transfer efficiency of probe **PPC**, an absorption spectrum of the acceptor and a fluorescence spectrum of the donor were measured (Fig. S11). The results showed that the absorption spectrum of the acceptor overlaid well with the fluorescence spectrum of the donor, implying high energy transfer efficiency could be expected. To further calculate energy transfer efficiency of probe **PPC** quantitatively, fluorescence intensities of probe **PPC** and the donor were measured in the same condition. Energy transfer efficiency (ETE) was calculated according to the following equation:

$$\eta_{ETE} = 1 - F_D/F_{DA}$$

Where, F_D denotes the maximum of fluorescence intensity of lone donor, and F_{DA} denotes the maximum of fluorescence intensity of the donor moiety in the probe. $\eta_{ETE} = 0.91$ implied high energy transfer efficiency of probe **PPC**.

The fluorescence quantum yield (Φ) was assessed by quinine sulfate as a standard and calculated by following equation:

$$\Phi = \Phi_s(IA_s/I_sA)(\eta^2/\eta_s^2)$$

Where, A denotes the absorbance, I denotes the integrated fluorescence intensity, η denotes the refractive index of the solvent. Φ of **PPC** and **PPC-S** were determined to be 0.233 and 0.392 respectively at room temperature.

3.6 Bioimaging of probe **PPC**

Encouraged by the excellent fluorescence properties of probe **PPC** for HOCl/OCl^-, we further studied the detection of intracellular HOCl/OCl^-. Firstly, we evaluated the practicability of probe **PPC** for the detection of HOCl/OCl^- in living cells (Fig. 3). After RAW264.7 macrophage cells were incubated with probe **PPC** (2 μM) for 30 min, strong fluorescence in the red channel and weak fluorescence in the blue channel were observed. After further incubation with various concentrations of HOCl/OCl^- for 30 min, the fluorescence in the red channel decreased and the fluorescence in the blue channel increased remarkably in a low concentrations range (0-5 μM). This proved that probe **PPC** could detect HOCl/OCl^- in living cells in a ratiometric fluorescence manner.

Fig. 3

Next, we investigated the suitability of probe **PPC** toward endogenous HOCl/OCl^- in RAW264.7 macrophage cells (Fig. 4). It is known that HOCl/OCl^- could be produced in cells by stimulating with LPS. In the experimental groups, macrophage cells were stimulated by LPS (1 μg/ml) for 12 h and then incubated with probe **PPC** (2 μM) for 30 min, the fluorescence from the red channel decreased and the fluorescence from the blue channel increased. In the control groups, without addition of LPS, obvious fluorescence in the red channel and faint fluorescence in the blue channel were obtained. The ratio of fluorescence intensity of blue channel and red channel (I_{blue}/I_{red}) increased remarkably in the presence of LPS. Therefore, probe **PPC** could successfully be used for the fluorescence imaging of endogenous and exogenous hypochlorite in RAW264.7 macrophage cells.

Fig. 4

The development of novel fluorescence probes for the selective detection of HOCl/OCl^- inside specific organelles is significant in biology and medical science. We evaluated the feasibility of probe **PPC** for sub-cellular localization. The fluorescence areas of probe **PPC** overlaid well with that of Mito Tracker Deep Red, and the co-localization coefficient is 0.94 (Fig. 5). Therefore, probe **PPC** could target mitochondria in RAW264.7 macrophage cells. The preferential distribution of probe **PPC** in mitochondria was unexpected. As we know, almost all mitochondria-targeted fluorescence probes had positive charge groups such as triphenylphosphonium (TPP) [38, 56] or pyridinium [57, 58]. Whereas, some neutral fluorescence probes for mitochondria had been focused on and developed [59-61]. Therefore, probe **PPC** probably was a second neutral mitochondria-targeted fluorescence probe for ratiometric detection of endogenous HOCl/OCl^-. Furthermore, probe **PPC** showed an excellent photostability (Fig. S12) and little cytotoxicity for living cells (Fig. S13).

Fig. 5

3.7 Investigation of the detecting mechanism

According to literature, the carbon-carbon double bond was more likely attacked by HOCl/OCl^- than the co-existed thioether group of phenothiazine [44]. Therefore, the decreased fluorescence of the acceptor moiety and the enhanced fluorescence of the donor unit may be attributed to the destruction of the carbon–carbon double bond (Scheme 2). To confirm our speculation, ^{1}H NMR titration of the reaction of probe **PPC** with HOCl/OCl^- were recorded (Fig. S14). With addition of increasing amount of HOCl/OCl^-, a signal peak of H_1 of probe **PPC** gradually decreased until disappeared and a signal peak of H_2 of **PPC-S** presented and reached the maximum. Therefore, **PPC-S** should be the product of probe **PPC** and HOCl/OCl^-. To further confirm our speculation,

three reaction solutions of probe **PPC** with 0, 3 and 7 equiv. $HOCl/OCl^-$ were evaluated by MS (Fig. S15). The strong peak at 645.2458 (m/z) corresponded to [**PPC** + H]$^+$ in MS spectrometry for the solution of probe **PPC** alone. Three peaks at 597.2414 (m/z), 619.2220 (m/z) and 645.2523 (m/z) corresponded to [**PPC-S** + H]$^+$, [**PPC-S** + Na]$^+$ and [**PPC** + H]$^+$ in MS spectrometry for the solution of probe **PPC** with 3 equiv. $HOCl/OCl^-$, respectively. A prominent peak at 597.2438 (m/z) and a minor peak at 619.2237 (m/z) corresponded to [**PPC-S** + H]$^+$ and [**PPC-S** + Na]$^+$ in MS spectrometry for the solution of probe **PPC** with 7 equiv. $HOCl/OCl^-$, respectively. Above data implied the gradual transformation of the probe **PPC** to **PPC-S**.

Conclusion

In summary, a ratiometric fluorescence probe **PPC** based on FRET mechanism with a large pseudo Stokes shift (209 nm) was developed for selective and sensitive detection of $HOCl/OCl^-$. The probe was successfully applied to the detection of exogenous and endogenous $HOCl/OCl^-$ in living RAW264.7 macrophage cells with good photostability and neglectable toxicity. Because of the excellent mitochondria-targeted ability, probe **PPC** can be competent in tracking of exogenous and endogenous $HOCl/OCl^-$ in mitochondria of living cells.

Acknowledgment

This study was supported by the National Key Research and Development Program of China (2017YFA0104604), the National Natural Science Foundation of China (No.31871407, 31741083，

31870831), the Natural Science Foundation of Shandong Province (ZR2018MB042).

References

[1] J.M. Zgliczynski, T. Stelmaszynska, W. Ostrowski, J. Naskalski, J. Sznajd, Myeloperoxidase of human leukaemic leucocytes oxidation of amino acids in the presence of hydrogen peroxide, Eur. J. Biochem., 4 (1968) 540-547.

[2] S. Khatib, R. Musa, J. Vaya, An exogenous marker: a novel approach for the characterization of oxidative stress, Bioorg. Med. Chem., 15 (2007) 3661-3666.

[3] S.A. Weitzman, L.I. Gordon, Inflammation and cancer: role of phagocyte-generated oxidants in carcinogenesis, Blood, 76 (1990) 655-663.

[4] S. Hammerschmidt, N. Büchler, H. Wahn, Tissue lipid peroxidation and reduced glutathione depletion in hypochlorite-induced lung injury, Chest, 121 (2002) 573-581.

[5] E. Malle, T. Buch, H.J. Grone, Myeloperoxidase in kidney disease, Kidney Int., 64 (2003) 1956-1967.

[6] A. Daugherty, J.L. Dunn, D.L. Rateri, J.W. Heinecke, Myeloperoxidase, a catalyst for lipoprotein oxidation, is expressed in human atherosclerotic lesions, J. Clin. Invest., 94 (1994) 437-444.

[7] J.E. Harrison, J. Schultz, Studies on the chlorinating activity of myeloperoxidase, J. Biol. Chem., 251 (1976) 1371-1374

[8] Y.W. Yap, M. Whiteman, N.S. Cheung, Chlorinative stress: an under appreciated mediator of neurodegeneration? Cell Signalling, 19 (2007) 219-228.

[9] Z.M. Prokopowicz, F. Arce, R. Biedron, C.L.L. Chiang, M. Ciszek, D.R. Katz, M. Nowakowska, S. Zapotoczny, J. Marcinkiewicz, B.M. Chain, Hypochlorous acid: a natural adjuvant that facilitates antigen processing, cross-priming, and the induction of adaptive immunity, The J. Immunology, 184 (2010) 824-835.

[10] W. Sun, J.L. Fan, C. Hu, J.F. Cao, H. Zhang, X.Q. Xiong, J.Y. Wang, S. Cui, S.G. Sun, X.J. Peng, A two-photon fluorescent probe with near-infrared emission for hydrogen sulfide imaging in biosystems, Chem. Commun., 49 (2013) 3890-3892.

[11] F.B. Yu, P. Li, P. Song, B.S. Wang, J.Z. Zhao, K.L. Han, Facilitative functionalization of cyanine dye by an on–off–on fluorescent switch for imaging of H_2O_2 oxidative stress and thiols reducing repair in cells and tissues, Chem. Commun., 48 (2012) 4980-4982.

[12] F.B. Yu, P. Li, P. Song, B.S. Wang, J.Z. Zhao, K.L. Han, An ICT-based strategy to a colorimetric and ratiometric fluorescence probe for hydrogen sulfide in living cells, Chem. Commun., 48 (2012) 2852-2854.

[13] Z.G. Lou, P. Li, X.F. Sun, S.Q. Yang, B.S. Wang, K.L. Han, A fluorescent probe for rapid detection of thiols and imaging of thiols reducing repair and H_2O_2 oxidative stress cycles in living cells, Chem. Commun., 49 (2013) 391-393.

[14] J. Yang, K. Li, J.T. Hou, C.Y. Lu, L.L. Li, K.K. Yu, X.Q. Yu, A novel coumarin-based water-soluble fluorescent probe for endogenously generated SO_2 in living cells, Sci. China Chem.,

60 (2017) 793-798.

[15] B.C. Zhu, Y.H. Xu, W.Q. Liu, C.X. Shao, H.F. Wu, H.L. Jiang, B. Du, X.L. Zhang, A highly selective colorimetric probe for fast and sensitive detection of hypochlorite in absolute aqueous solution, Sens. Actuators B, 191 (2014) 473-478.

[16] Y. Liu, K. Li, K.X. Xie, L.L. Li, K.K. Yu, X. Wang, X.Q. Yu, A water-soluble and fast-response mitochondria targeted fluorescent probe for colorimetric and ratiometric sensing of endogenously generated SO_2 derivatives in living cells, Chem. Commun., 52 (2016) 3430-3433.

[17] L. Yang, Y.N. Su, Z.K. Sha, Y.N. Geng, F.P. Qia, X.Z. Song, A red-emitting fluorescent probe for hydrogen sulfide in living cells with a large Stokes shift, Org. Biomol. Chem., 16 (2018) 1150-1156.

[18] G.H. Cheng, J.L. Fan, W. Sun, J.F. Cao, C. Hu, X.J. Peng, A near-infrared fluorescent probe for selective detection of HClO based on Se-sensitized aggregation of heptamethine cyanine dye, Chem. Commun., 50 (2014) 1018-1020.

[19] B.S. Wang, Peng Li, F. Yu, J. Chen, Z. Qu, K. Han, A near-infrared reversible and ratiometric fluorescent probe based on Se-BODIPY for the redox cycle mediated by hypobromous acid and hydrogen sulfide in living cells, Chem. Commun., 49 (2013) 5790-5792.

[20] B.S. Wang, P. Li, F.B. Yu, P. Song, X.F. Sun, S.Q. Yang, Z.G. Lou, K.L. Han, A reversible fluorescence probe based on Se–BODIPY for the redox cycle between HClO oxidative stress and H_2S repair in living cells, Chem. Commun., 49 (2013) 1014-1016.

[21] J.T. Hou, K. Li, J. Yang, K.K. Yu, Y.X. Liao, Y.Z. Ran, Y.H. Liu, X.D. Zhou, X.Q. Yu, A ratiometric fluorescent probe for in situ quantification of basal mitochondrial hypochlorite in cancer cells, Chem. Commun., 51 (2015) 6781-6784.

[22] J. Yang, K. Li, J.T. Hou, L.L. Li, C.Y. Lu, Y.M. Xie, X. Wang, X.Q. Yu, Novel tumor-specific and mitochondria-targeted near-infrared emission fluorescent probe for SO_2 derivatives in living cells, ACS Sens., 51 (2016) 166-172.

[23] K. Li, J.T. Hou, J. Yang, X.Q. Yu, A tumor-specific and mitochondria-targeted fluorescent probe for real-time sensing of hypochlorite in living cells, Chem. Commun., 53 (2017) 5539-5541.

[24] J.T. Hou, M.Y. Wu, K. Li, J. Yang, K.K. Yu, Y. M. Xie, X.Q. Yu, Mitochondria-targeted colorimetric and fluorescent probes for hypochlorite and their applications for in vivo imaging, Chem. Commun., 50 (2014) 8640-8643.

[25] F. Liu, T. Wu, J.F. Cao, H. Zhang, M.M. Hu, S.G. Sun, F.L. Song, J.L. Fan, J.Y. Wang, X.J. Peng, A novel fluorescent sensor for detection of highly reactive oxygen species, and for imaging such endogenous hROS in the mitochondria of living cells, Analyst, 138 (2013) 775-778.

[26] M. Vedamalai, D. Kedaria, R. Vasita, I. Gupta, Oxidation of phenothiazine based fluorescent probe for hypochlorite and its application to live cell imaging, Sens. Actuators B, 263 (2018) 137-142.

[27] B.C. Zhu, H.L. Jiang, B.P. Guo, C.X. Shao, H.F. Wu, B. Du, Q. Wei, A highly selective ratiometric fluorescent probe for hydrogen peroxide displaying a large emission shift, Sens. Actuators B, 186 (2013) 681-686.

[28] Y.L. Pak, S.J. Park, Q. Xu, H.M. Kim, J. Yoon, Ratiometric two-photon fluorescent probe for

detecting and imaging hypochlorite, Anal. Chem. 90 (2018) 9510-9514.

[29] Y.R. Zhang, X.P. Chen, J. Shao, J.Y. Zhang, Q. Yuan, J.Y. Miao, B.X. Zhao, A ratiometric fluorescent probe for sensing HOCl based on a coumarine-rhodamine dyad, Chem. Commun., 50 (2014) 14241-14244.

[30] Y. Liu, Z.M. Zhao, J.Y. Miao, B.X. Zhao, A ratiometric fluorescent probe based on boron dipyrromethene and rhodamine Förster resonance energy transfer platform for hypochlorous acid and its application in living cells, Anal. Chim. Acta, 921 (2016) 77-83.

[31] W.L. Wu, H.L. Ma, M.F. Huang, J.Y. Miao, B.X. Zhao, Mitochondria-targeted ratiometric fluorescent probe based on FRET for bisulfite, Sens. Actuators B, 241 (2017) 239-244

[32] W.L. Wu, X. Zhao, L.L. Xi, M.F. Huang, W.H. Zeng, J.Y. Miao, B.X. Zhao, A mitochondria-targeted fluorescence probe for ratiometric detection of endogenous hypochlorite in the living cells, Anal. Chim. Acta, 950 (2017) 178-183

[33] X. Han, L. Zhao, D.E. Wang, J. Xu, L.l. Zhang, M.S. Yuan, Q. Tu, J.Y. Wang, A TBET-based ratiometric probe for Au^{3+} and its application in living cells, Analyst, 141 (2016) 1098-1104.

[34] U.R. G., V. Ramu, S. Roy, N. Taye, S. Chattopadhyay, A. Das, A specific probe for Hg^{2+} to delineate even H^{+} in pure aqueous buffer/Hct116 colon cancer cells: Hg(II)- η^{2}-arene π-interaction and a TBET-based fluorescence response, Chem. Commun., 50 (2014) 14421-14424.

[35] W.Q. Chen, X.X. Yue, H. Zhang, W.X. Li, L.L. Zhang, Q. Xiao, C.S. Huang, J.R. Sheng, X.Z. Song, Simultaneous detection of glutathione and hydrogen polysulfides from different emission channels, Anal. Chem., 89 (2017) 12984-12991.

[36] P. Hou, S. Chen, H.B. Wang, J.X. Wang, K. Voitchovsky, X.Z. Song, An aqueous red emitting fluorescent fluoride sensing probe exhibiting a large Stokes shift and its application in cell imaging,

Chem. Commun., 50 (2014) 320-322.

[37] X.J. Liu, L. He, L.Yang, Y.N. Geng, L. Yang, X.Z. Song, Iminocoumarin-based fluorescence probe for intracellular H_2O_2 detection with a red emission and a large Stokes shift, Sens. Actuators B, 259 (2018) 803-808.

[38] G.H. Cheng, J.L. Fan, W. Sun, K. Sui, X. Jin, J.Y. Wang, X.J. Peng, A highly specific BODIPY-based probe localized in mitochondria for HClO imaging, Analyst, 138 (2013) 6091-6096.

[39] D.P. Li, Z.Y. Wang, X.J. Cao, J. Cui, X. Wang, H.Z. Cui, J.T. Miao, B.X. Zhao, A mitochondria-targeted fluorescent probe for ratiometric detection of endogenous sulfur dioxide derivatives in cancer cells, Chem. Commun., 52 (2016) 2760-2763.

[40] J.W. Reed, H.H. Ho, W.L. Jolly, Chemical synthesis with a quenched flow reactor. hydroxytrihydroborate and peroxynitrite, J. Am. Chem. Soc., 96 (1974) 1248-1249

[41] Z. Ma, W. Sun, L.Z. Chen, J. Li, Z.Z. Liu, H.X. Bai, M.Y. Zhu, L.P. Du, X.D. Shi, M.Y. Li, A novel hydrazino-substituted naphthalimide-basedfluorogenic probe for tert-butoxy radicals, Chem. Commun., 49 (2013) 6295-6297.

[42] X. Li, G. Zhang, H. Ma, D. Zhang, J. Li, D. Zhu, 4,5-Dimethylthio-4-[2-(9-anthryloxy)ethylthio]tetrathiafulvalene, a highly selective and sensitive chemiluminescence probe for singlet oxygen, J. Am. Chem. Soc., 126 (2004) 11543-11548.

[43] W.L. Wu, Z.Y. Wang, X. Dai, J.Y. Miao, B.X. Zhao, An effective colorimetric and ratiometric fluorescent probe based FRET with a large Stokes shift for bisulfite, Scientific Reports, 6 (2016) 25315.

[44] H.D. Xiao, J.H. Li, J. Zhao, G. Yin, Y.W. Quan, J. Wang, R.Y. Wang, A colorimetric and ratiometric fluorescent probe for ClO^- targeting in mitochondria and its application in vivo, J. Mater.

Chem. B, 3 (2015) 1633-1638.

[45] J.Y. Zha, B.Q. Fu, C.Q. Qin, L.T. Zeng, X.C. Hu, A ratiometric fluorescent probe for rapid and sensitive visualization of hypochlorite in living cells, RSC Adv., 4 (2014) 43110-43113.

[46] L. Yuan, W.Y. Lin, J.Z. Song, Y.T. Yang, Development of an ICT-based ratiometric fluorescent hypochlorite probe suitable for living cell imaging, Chem. Commun., 47 (2011) 12691-12693.

[47] L. Wang, L.L. Long, L.P. Zhou, Y.J. Wu, C. Zhang, Z.X. Han, J.L. Wang, Z.L. Da, A ratiometric fluorescent probe for highly selective and sensitive detection of hypochlorite based on the oxidation of N-alkylpyridinium, RSC Adv., 4 (2014) 59535-59540.

[48] W. Shu, P. Jia, X.Z. Chen, X.Y. Li, Y.R. Huo, F. Liu, Z.K. Wang, C.Y. Liu, B.C. Zhu, L.G. Yan, B. Du, A highly selective ratiometric fluorescent probe for the sensitive detection of hypochlorous acid and its bioimaging applications, RSC Adv., 6 (2016) 64315-64322

[49] S. Goswami, K. Aich, S. Das, B. Pakhira, K. Ghoshal, C.K. Quah, M. Bhattacharyya, H.K. Fun, S. Sarkar, A triphenyl amine-based solvatofluorochromic dye for the selective and ratiometric sensing of OCl^-, in human blood cells, Chem. Asian J., 10 (2015) 694-700.

[50] Y.R. Zhang, N. Meng, J.Y. Miao, B.X. Zhao, A ratiometric fluorescent probe based on a through-bond energy transfer (TBET) system for imaging HOCl in living cells, Chem. Eur. J., 21 (2015) 19058-19063

[51] Y.R. Zhang, Z.M. Zhao, J.Y. Miao, B.X. Zhao, A ratiometric fluorescence probe based on a novel FRET platform for imaging endogenous HOCl in the living cells, Sens. Actuators B, 229 (2016) 408-413.

[52] S.S. Ding, Q. Zhang, S.H. Xue, G.Q. Feng, Real-time detection of hypochlorite in tap water and biological samples by a colorimetric, ratiometric and near-infrared fluorescent turn-on probe, Analyst,

140 (2015) 4687-4693.

[53] W.Y. Lin, L.L. Long, B.B. Chen, W. Tan, A Ratiometric fluorescent probe for hypochlorite based on a deoximation reaction, Chem. Eur. J., 15 (2009) 2305-2309.

[54] L.L. Long, D.D. Zhang, X.F. Li, J.F. Zhang, C. Zhang, L.P. Zhou, A fluorescence ratiometric sensor for hypochlorite based on a novel dual-fluorophore response approach, Anal. Chim. Acta, 775 (2013) 100-105.

[55] Y.L. Pak, S.J. Park, D. Wu, B.H. Cheon, H.M. Kim, J. Bouffard, J.Y. Yoon, *N*-Heterocyclic carbene boranes as reactive oxygen species responsive materials: Application to the two-photon imaging of hypochlorous acid in living cells and tissues, Angew. Chem. Int. Ed., 57 (2018) 1567-1571.

[56] L. Yuan, L. Wang, B.K. Agrawalla, S. Park, H. Zhu, B. Sivaraman, J. Peng, Q.H. Xu and Y.T. Chang, Development of targetable two-photon fluorescent probes to image hypochlorous acid in mitochondria and lysosome in live cell and inflamed mouse model, J. Am. Chem. Soc., 137 (2015) 5930-5938.

[57] H. Zhang, J. Liu, Y. Q. Sun, Y. Huo, Y. Li, W. Liu, X. Wu, N. Zhu, Y. Shi, W. Guo, A mitochondria-targetable fluorescent probe for peroxynitrite: fast response and high selectivity, Chem. Commun., 51 (2015) 2721-2724.

[58] Y. Chen, C. Zhu, Z. Yang, J. Chen, Y. He, Y. Jiao, W. He, L. Qiu, J. Cen, Z. Guo, A ratiometric fluorescent probe for rapid detection of hydrogen sulfide in mitochondria, Angew. Chem. Int. Ed., 52 (2013) 1688-1691.

[59] Y.Y. Cheng, G.C. Li, Y. Liu, Y. Shi, G. Gao, D. Wu, J.B. Lan, J.S. You, Unparalleled ease of

access to a library of biheteroaryl fluorophores via oxidative cross-coupling reactions: discovery of photostable NIR probe for mitochondria, J. Am. Chem. Soc., 138 (2016) 4730-4738.

[60] Y. Kawazoe, H. Shimogawa, A. Sato, M. Uesugi, A Mitochondrial surface-specific fluorescent probe activated by bioconversion, Angew. Chem. Int. Ed., 50 (2011) 5478-5481.

[61] S. Zhang, J. Fan, S. Zhang, J. Wang, X. Wang, J. Du, X. Peng, Lighting up fluoride ions in cellular mitochondria using a highly selective and sensitive fluorescent probe, Chem. Commun., 50 (2014) 14021-14024.

Legend of figures

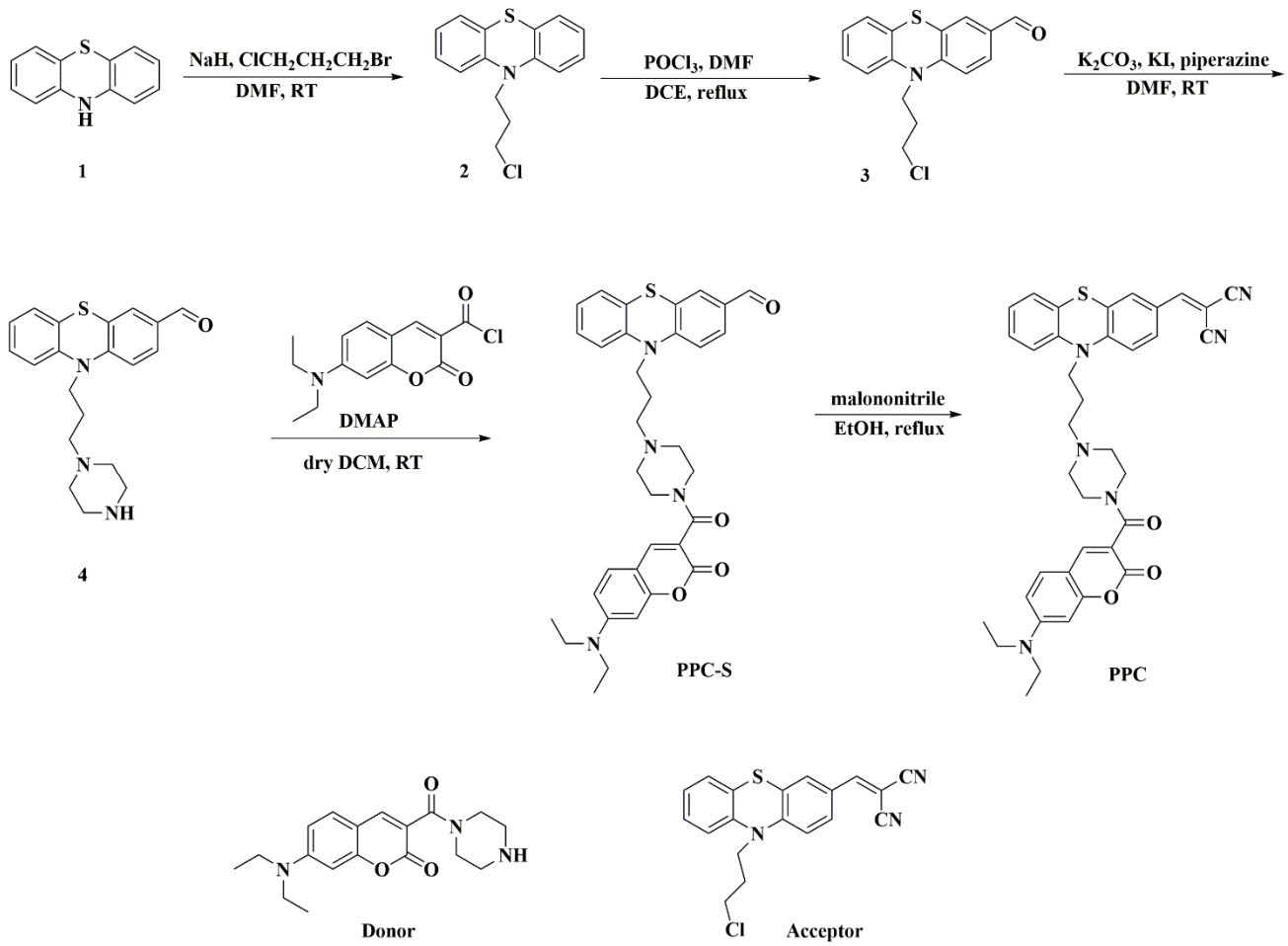

Scheme 1 Synthesis of probe **PPC**

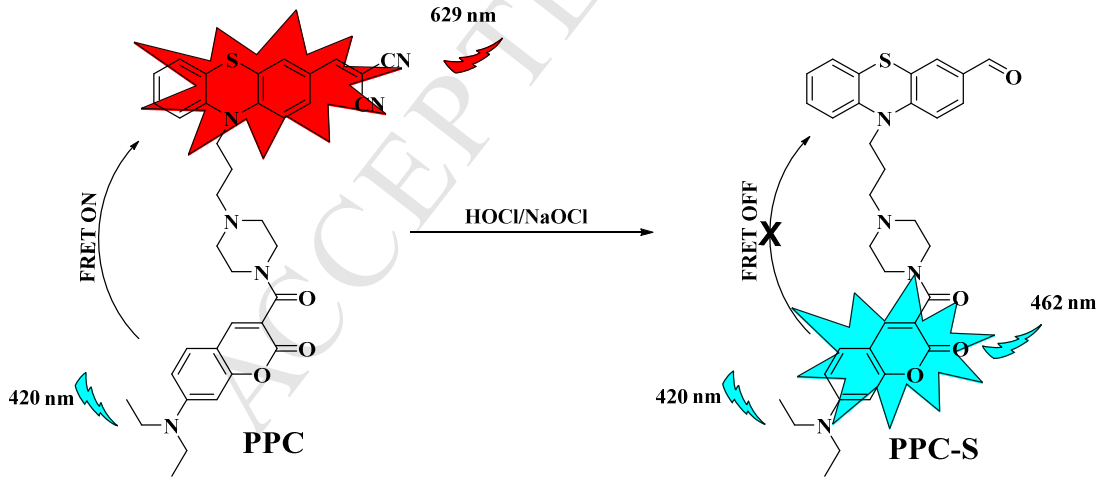

Scheme 2 The proposed detection mechanism of probe **PPC** for $HOCl/OCl^-$.

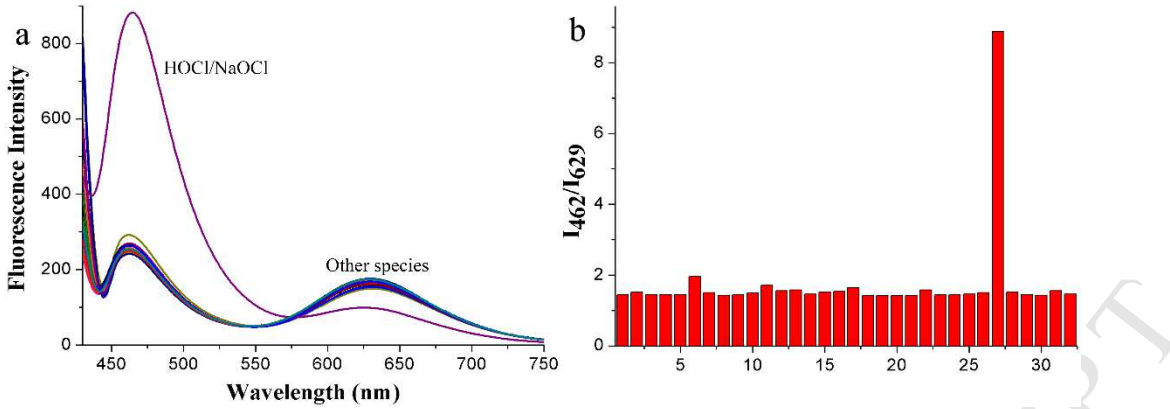

Fig. 1 (a) Fluorescence spectra of probe **PPC** (5 μM) in the presence of HOCl/OCl^- (6 equiv.) and other analytes (25 equiv., vacant, H_2O_2, KO_2, NO, $^1O_2$, *t*-BuOOH, *t*-BuOO•, •OH, $ONOO^-$, Na^+, Al^{3+}, Zn^{2+}, Ca^{2+}, Fe^{3+}, Fe^{2+}, Cu^{2+}, Mg^{2+}, F^-, Cl^-, Br^-, I^-, CO_3^{2-}, SO_4^{2-}, NO_2^-, AcO^-, HPO_3^{2-}, HOCl/OCl^-, Cys, GSH, Hcy, H_2S and HSO_3^-) in PBS (pH = 7.4, 10 mM with 1 mM Triton X-100). (b) Response (I_{462}/I_{629}) of probe **PPC** toward analytes in PBS (pH = 7.4, 10 mM with 1 mM Triton X-100). 1. Vacant; 2. H_2O_2; 3. KO_2; 4. NO; 5. $^1O_2$; 6. *t*-BuOOH; 7. *t*-BuOO•; 8. •OH; 9. $ONOO^-$; 10. Na^+; 11. Al^{3+}; 12. Zn^{2+}; 13. Ca^{2+}; 14. Fe^{3+}; 15. Fe^{2+}; 16. Cu^{2+}; 17. Mg^{2+}; 18. F^-; 19. Cl^-; 20. Br^-; 21. I^-; 22. CO_3^{2-}; 23. SO_4^{2-}; 24. NO_2^-; 25. AcO^-; 26. HPO_3^{2-}; 27. HOCl/OCl^-, 28. Cys, 29. GSH, 30. Hcy, 31. H_2S, 32. HSO_3^-. λ_{ex} = 420 nm.

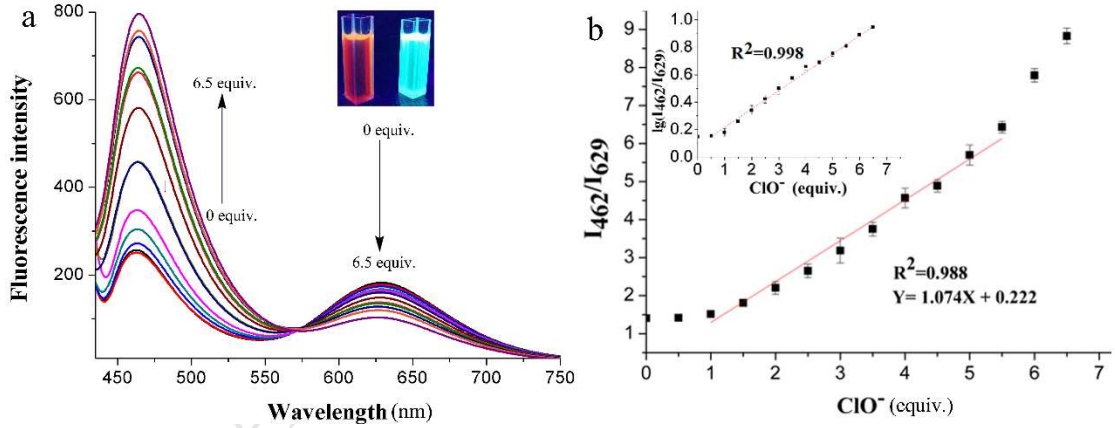

Fig. 2 (a) Fluorescence spectra of probe **PPC** (5 μM) in the presence of different concentrations of HOCl/OCl^- (0, 0.5, 1, 1.5, 2, 2.5, 3, 3.5, 4, 4.5, 5, 5.5, 6, 6.5 equiv.) in PBS (pH = 7.4, 10 mM with 1 mM triton X-100), (λ_{ex} = 420 nm, slit: 15 nm/7 nm). Inset: A visual fluorescence changed from red to blue under illumination using a 365 nm UV lamp. (b) I_{462}/I_{629} changes with the addition of HOCl/OCl^- (0, 0.5, 1, 1.5, 2, 2.5, 3, 3.5, 4, 4.5, 5, 5.5, 6, 6.5 equiv.). Inset: lg(I_{462}/I_{629}) changes with the addition of HOCl/OCl^- (0, 0.5, 1, 1.5, 2, 2.5, 3, 3.5, 4, 4.5, 5, 5.5, 6, 6.5 equiv.)

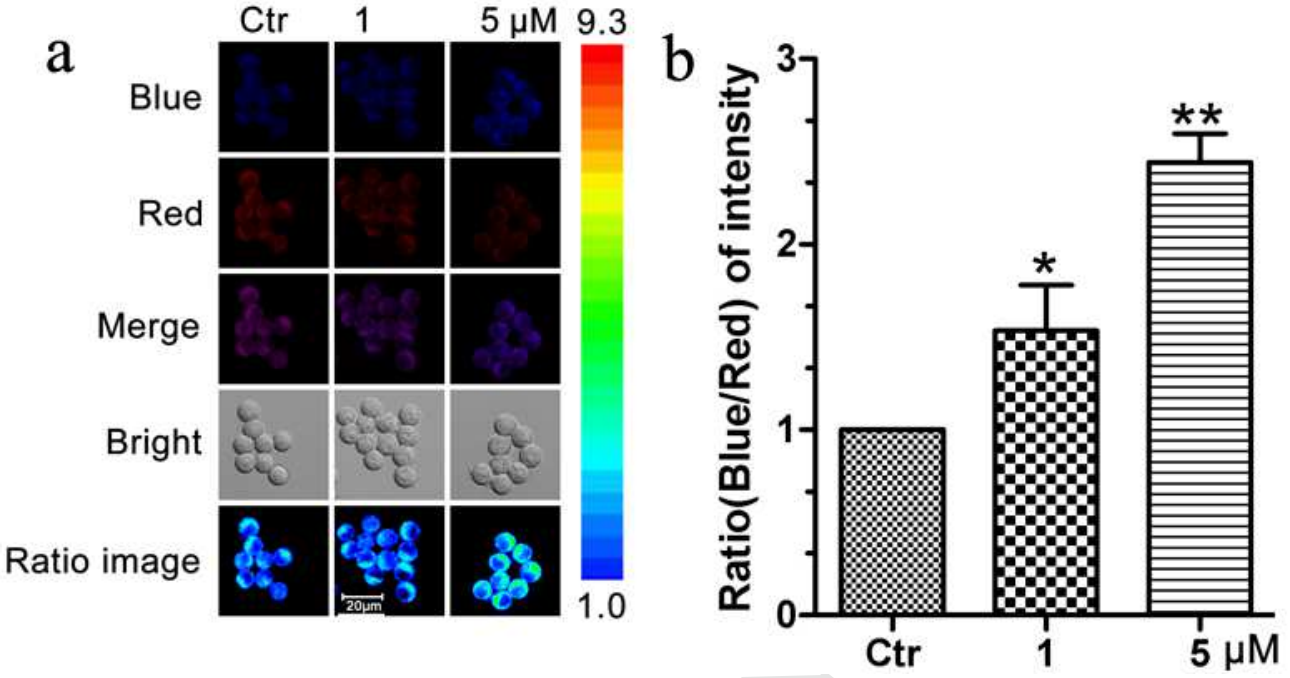

Fig. **3** (a) Confocal fluorescence images of RAW 264.7 cells pretreated with different concentrations of HOCl/OCl¯(0, 1, 5 μM) and then incubated with probe **PPC** (2 μM) for 30 min. (b) The relative ratio (blue/red) of fluorescence intensity.

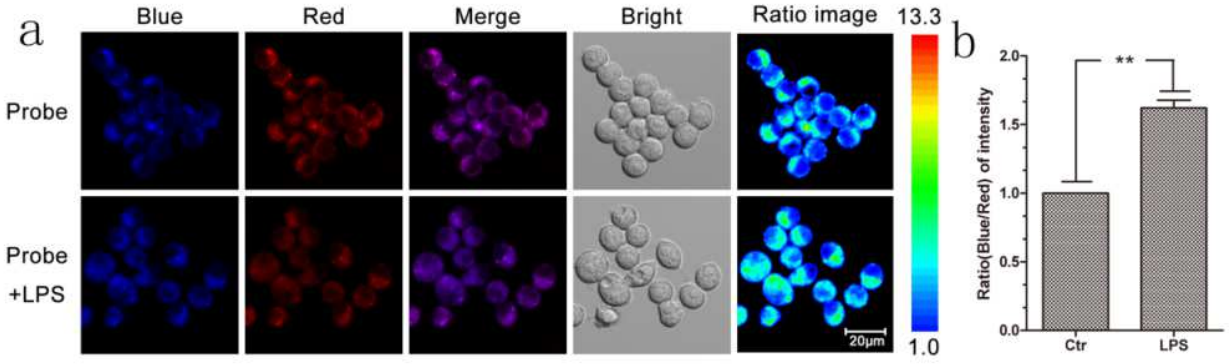

Fig. 4 (a) The first row (horizontally): Fluorescence and bright field images of RAW264.7 cells incubated with probe **PPC** (2 μM) for 30 min. The second row (horizontally): Fluorescence and bright field images of RAW264.7 cells stimulated by LPS (1μg/ml) for 12 h and then incubated with probe **PPC** (2 μM) for 30 min. (b) Ratio (blue/red) of fluorescence intensity.

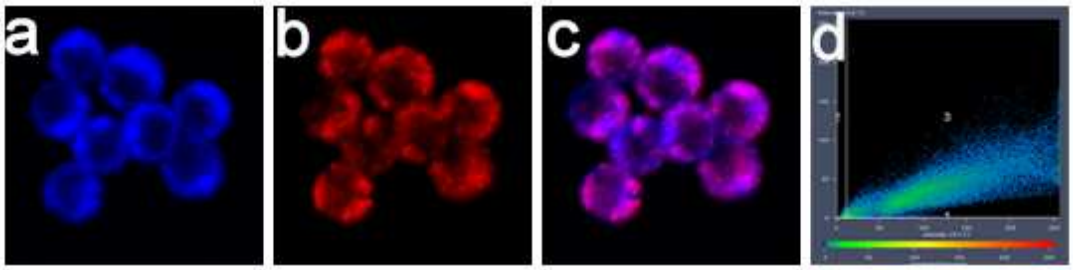

Fig. 5 RAW264.7 cells were incubated with probe **PPC** (2 μM) for 30 min, followed by Mito Tracker Deep Red for 30 min. (a) The cell image of probe **PPC**, λ_{ex} = 405 nm, λ_{em} = 405-550 nm. (b) The cell image of Mito Tracker Deep Red, λ_{ex} = 639 nm, λ_{em} = 640-700 nm. (c) Merged image. (d) The co-localization coefficient (Pearson's coefficient) of probe **PPC** and Mito Tracker Deep Red was 0.94.

Highlights

- A novel ratiometric fluorescent probe (named PPC) for hypochlorite based on FRET platform was developed.
- PPC showed a large pseudo Stokes shift (209 nm), high selectivity, sensitivity and fast response.
- PPC could target well mitochondria in cell image.
- PPC could image endogenous hypochlorite in RAW264.7 cells.